Inorganic Chemistry

Article

pubs.acs.org/IC

Interactions of Octahedral Ruthenium(II) Polypyridyl Complexes with the RNA Triplex poly(U)•poly(A)*poly(U) Effect on the Third-Strand Stabilization

Xiao-Jun He and Li-Feng Tan*

Key Lab of Environment-Friendly Chemistry and Application in Ministry of Education, Xiangtan University, Xiangtan 411105, PR China

Supporting Information

ABSTRACT: Stable triplexes play key roles in many biological processes. Due to the Hoogsteen base pairing, triplexes are, however, thermodynamically less stable than the corresponding duplexes. The poor stabilization of these structures limits their practical applications under physiological conditions. To understand the factors effect on the stabilization of RNA triplexes by octahedral ruthenium(II) complexes, the interactions of $[RuL_2(uip)]^{2+}$ {where L = 2,2′-bipyridine (bpy) or 1,10-phenanthroline phen, uip = 2-(5-uracil)-1*H*-imidazo[4,5-*f*][1,10]phenanthroline} with the RNA triplex poly(U)•poly(A)*poly(U) are examined by spectrophotometry, spectrofluorometry, circular dichroism, and viscosimetry in this work. The main results obtained here suggest that the third-strand stabilization depends on the hydrophobicity effects of ancillary ligands bpy and phen.

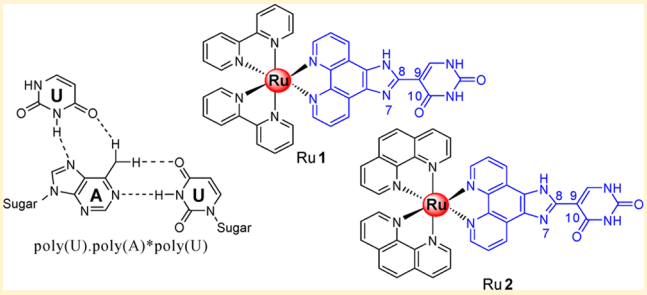

INTRODUCTION

Nucleic acid triple helical structures (also called triplexes) were originally discovered by Rich and co-workers as early as in 1957.[1] Subsequently, both triple-strand DNA-type and RNA-type structures have been prepared and studied by several teams.[2] These structures, however, had not been given biological relevance until the triple helix regions were found to exist in H-DNA.[3] After that, there has been renewed interest in investigating triple helices because these novel structures have been implicated as a possible means of controlling cellular processes by endogenous or exogenous mechanisms,[4−11] such as post-transcriptional RNA processing, modification of chromatin antigene therapy, and gene regulation. More recently, the potential in vivo functions of triple helices have been reviewed in detail by Prof. Bailey and co-workers, which opens up new vistas in understanding genome biology and gene regulation based on triple helices.[12]

Stable triplexes play key roles in many biological processes.[6] Due to the Hoogsteen base pairing, triple helices are, however, thermodynamically less stable than the corresponding duplexes. For example, concerning the RNA triplex poly(U)•poly(A)*poly(U) (Figure 1, where • denotes the Watson−Crick base pairing and * denotes the Hoogsteen base pairing), the third strand poly(U) separation from the triplex structure occurs at about 37 °C, whereas the duplex strand poly(U)•poly(A) separation occurs around 47 °C.[13] The poor stability of these structures limits their practical use under physiological conditions.[6,12,14] In this regard, small molecules able to recognize, bind, and stabilize the specific sequences of triple helices are of importance.[14,15]

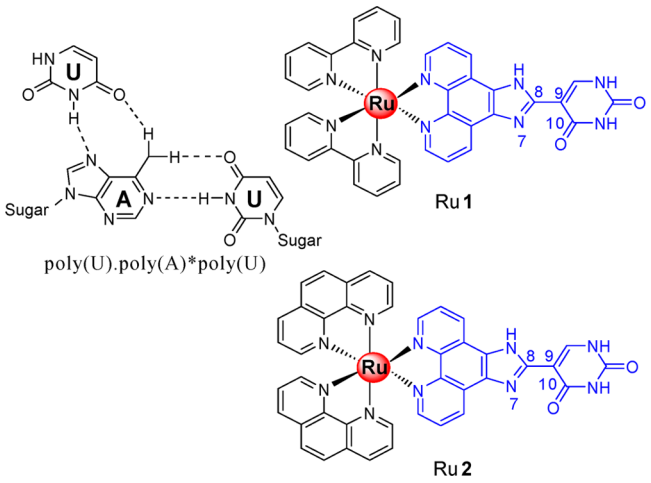

Figure 1. Chemical structures of $[Ru(bpy)_2(uip)]^{2+}$ (Ru**1**), $[Ru(phen)_2(uip)]^{2+}$ (Ru**2**), and the base pairing scheme in RNA triplex.

In recent years, many efforts have been initiated to use natural and synthetic small molecules to modulate the properties of triplex structures.[16] Surprisingly and in contrast to DNA triple helices, however, investigations of the stabilization of RNA triple helices by small molecules at present are less well established. Furthermore, most of these studies are limited to organic compounds[17−23] and, to a far

Received: July 21, 2014
Published: October 1, 2014

   dx.doi.org/10.1021/ic5017565 | *Inorg. Chem.* 2014, 53, 11152−11159

lesser extent, on metal complexes.[19c,24] The stabilization of RNA triple helices can be achieved by the action of intercalators,[25] in particular, when covalently linked to the third strand.[26] However, intercalators not covalently linked can either stabilize or destabilize RNA triplexes.[16a,17] For example, the melting experiments reveal that ethidium,[19a] proflavine (PR), and its platinum(II)-proflavine complex (PtPR)[19c] tend to destabilize the triplex, whereas berberine analogs[20b] are able to strongly stabilize the Hoogsteen base-paired third strand of RNA triplexes by intercalation. In addition, some alkaloids stabilize the Hoogsteen base-paired third strand of RNA triplexes almost without affecting the stability of the duplex, such as berberine, palmatine, and coralyne.[25a] These studies reflect that the effect of the intercalative process and modes on the stability of RNA triple helices is more complicated than previously thought and very sensitive to the structure of the bound compound. In our quest for small molecules for triple helix stabilization, we recently reported that the ruthenium(II) polypyridyl complex, $[Ru(phen)_2(mdpz)]^{2+}$ {phen = 1,10-phenanthroline; mdpz = 7,7′-methylenedioxyphenyl-dipyrido-[3,2-*a*:2′,3′-*c*]-phen-azine}, may serve as a prominent molecular "light switch" for poly(U)•poly(A)*poly(U) and stabilizes it by intercalation.[27]

It is well established that octahedral ruthenium(II) polypyridyl complexes, due to a combination of easily constructed rigid chiral structures spanning all three spatial dimensions and a rich photophysical repertoire, prominent DNA binding properties, and promising biological activity, have attracted considerable attention in recent years.[28] However, interactions of octahedral ruthenium(II) polypyridyl complexes with triplexes have come to the forefront.[27,29] Recently, Ji and his co-workers reported that a Ru(II) polypyridyl complex $[Ru(bpy)_2(uip)]^{2+}$ (Figure 1; bpy = 2,2′-bipyridine, uip = 2-(5-uracil)-1*H*-imidazo[4,5-*f*][1,10]phenanthroline) not only could intercalate into CT-DNA base pairs with high affinity, but also could bind with DNA topoisomerase II directly.[30] What about the binding behavior of this complex with triplexes? This will be discussed in this paper.

To understand the effect of the factors on the stabilization of RNA triplexes by octahedral ruthenium(II) complexes, $[Ru(bpy)_2(uip)]^{2+}$ (Ru**1**) is chosen in this work for study. For comparison with Ru**1**, a new complex, $[Ru(phen)_2(uip)]^{2+}$ (Ru**2**, Figure 1) has been synthesized and characterized. Interactions of the two metal complexes with the RNA triplex poly(U)•poly(A)*poly(U) are examined by spectrophotometry, spectrofluorometry, circular dichroism, and viscosimetry.

EXPERIMENTAL SECTION

Materials and Chemicals. Uip and *cis*-$[Ru(bpy)_2(uip)](ClO_4)_2$,[30] 1,10-phenanthroline-5,6-dione,[31] *cis*-$[Ru(phen)_2Cl_2]\cdot 2H_2O$, and *cis*-$[Ru(bpy)_2Cl_2]\cdot 2H_2O$[32] were prepared according to literature procedures. Polynucleotide samples of double-stranded poly(A)•poly(U) and single-stranded poly(U) were obtained from Sigma-Aldrich Corporation (St. Louis, MO, USA) and were used as received. Formation of the triplex poly(U)•poly(A)*poly(U) was carried out as reported earlier.[33] The concentration of poly(U)•poly(A)*poly(U) was determined optically using molar extinction coefficients, ε (M^{-1} cm^{-1}) reported in the literature.[13,33,34] All titration experiments were conducted at 20 °C in pH 7.0 phosphate buffer (6 mmol/L Na_2HPO_4, 2 mmol/L NaH_2PO_4, 1 mmol/L Na_2EDTA, 19 mmol/L NaC1). All reagents and solvents were purchased commercially and used without further purification unless specially noted, and ultrapure water was used in all experiments.

Microanalyses (C, H, and N) were carried out on a Perkin–Elmer 240Q elemental analyzer. ^1H NMR spectra were recorded on an Avance-400 spectrometer with d_6-DMSO as solvent at room temperature and TMS (tetramethylsilane) as the internal standard. Mass spectrometry was performed on an Autoflex III Maldi-Tof mass spectrometer (Bruker) using DMSO as the mobile phase.

Synthesis of *cis*-$[Ru(phen)_2(uip)](ClO_4)_2\bullet H_2O$(Ru2). A mixture of *cis*-$[Ru(phen)_2Cl_2]\cdot 2H_2O$ (210 mg, 0.4 mM), uip (150 mg, 0.4 mM), and ethylene glycol (18 mL) was thoroughly deoxygenated. The mixture was heated for 9 h at 150 °C under argon to give a dark red solution. The solution was cooled to room temperature and an equal volume of saturated aqueous sodium perchlorate solution was added under vigorous stirring. The red solid was collected and washed with small amounts of water, ethanol, and diethyl ether, respectively, and then dried under vacuum and purified on a neutral alumina column with MeCN–toluene (6:1, v/v) as eluant. Yield: 189 mg, 60%. Anal. Calcd for $C_{41}H_{26}N_{10}Cl_2O_{10}Ru\cdot H_2O$: C, 48.92; H, 2.80; N, 15.30. Found: C, 48.85; H, 2.92; N, 15.26. Maldi-Tof-MS (MeCN, *m*/*z*): 791.1 ($[M]^{2+}$), 891.1 ($[M+ClO_4^-]^+$). UV λ_{max}/nm (ε/M^{-1} cm^{-1}, MeCN): 454 (24600), 264 (127900). ^1H NMR (ppm, DMSO-d_6): 13.68 (s, 1H), 11.79 (d, *J* = 16, 1H), 9.44 (d, *J* = 8.0, 2H), 9.01 (d, *J* = 8.0, 1H), 8.76 (d, *J* = 8.0, 4H), 8.42 (d, *J* = 8.0, 2H), 8.38 (s, 4H), 8.06 (d, *J* = 8.0, 4H), 8.00 (t, 2H), 7.96 (t, 2H), 7.75 (t, 2H).

Electronic Absorption Spectral Studies. UV–vis spectra were collected using an Agilent spectrum Cary 100 spectrophotometer at 20 °C. A typical titration of each metal complex in phosphate buffer was performed by fixing the metal complex concentration, to which the RNA triplex stock solution is gradually added up to saturation. After each addition, the solution should be mixed evenly and allowed to re-equilibrate for at least 3 min before recording the absorption spectra. The intrinsic binding constant K_b and the binding site *s* of each metal complex toward the triplex from absorbance titrations are calculated by the following equation:[35]

$$\frac{\varepsilon_a - \varepsilon_f}{\varepsilon_b - \varepsilon_f} = \frac{\sqrt{b - (b^2 - 2K_b{}^2C_t[\mathrm{RNA}]/s)}}{2K_bC_t} \quad (1a)$$

$$b = \frac{1 + K_bC_t + K_b[\mathrm{RNA}]}{2s} \quad (1b)$$

where [RNA] is the concentration of poly(U)•poly(A)*poly(U) in the nucleotide phosphate and ε_a, ε_f, and ε_b, respectively, are the apparent, free, and bound metal complex extinction coefficients. K_b is the equilibrium binding constant in M^{-1}, C_t is the total metal complex concentration, and *s* is the average binding size.

Luminescence Titration with the RNA Triplex. Luminescence titrations was carried out a PTI Qm400 luminescence spectrometer at 20 °C, and a dilute solution of either Ru**1** or Ru**2** (2 uM) in phosphate buffer was excited at 470 nm. After each addition of the RNA triplex, the solution was mixed evenly and allowed to re-equilibrate for at least 3 min before recording the curve.

Fluorescence Quenching of the Metal Complex-Triplex System with $[Fe(CN)_6]^{4-}$. Fluorescence quenching experiments were carried out with the anionic quencher $[Fe(CN)_6]^{4-}$ at 20 °C. For each measurement in addition to the normal buffer components, different volume of KCl solution is added to keep the total ionic strength of the system at a constant. The data are plotted as Stern–Volmer plots of relative fluorescence intensity (I_0/I) versus [Q] according to the Stern–Volmer equation[36]

$$I/I_0 = 1 + K_{sv}[\mathrm{Q}]$$

where I_0 and I denote the fluorescence emission intensities in the absence and presence of the quencher and [Q] stands for $[Fe(CN)_6]^{4-}$ concentration. K_{sv} is the Stern–Volmer quenching constant.

Determination of the Binding Mode by Viscosity Studies. Viscosity measurements were carried out using an Ubbelohde viscometer maintained at a constant temperature of (20 ± 0.1) °C in a thermostatic bath. The flow time was measured with a digital stopwatch, and each sample was measured three times to get an

dx.doi.org/10.1021/ic5017565 | *Inorg. Chem.* 2014, 53, 11152–11159

average calculated time. Relative viscosities for the triplex RNA in either the absence or presence of metal complexes were calculated according to literature procedures reported earlier.[37]

Conformational Aspects of the Binding. Circular dichroic spectrum of the RNA triplex in the absence and presence of each metal complex was performed with a Jasco-810 spectropolarimeter at 20 °C. After each addition of the metal complex, the solution was mixed evenly and allowed to re-equilibrate for at least 5 min before recording the CD spectra. Each spectrum was averaged from three successive accumulations and was baseline-corrected, smoothed, and normalized to nucleotide phosphate concentration in the region 200−600 nm using the software supplied by Jasco.

Thermal Denaturation Studies. Thermal RNA denaturation experiments were carried out with an Agilent spectrum Cary 100 spectrophotometer equipped with a Cary 100 temperature-control programmer (±0.1 °C). The temperature of the solution was increased from 25 to 65 °C at a rate of 1.0 °C min^{-1}, and the absorbance at about 260 nm was continuously monitored for solutions of the RNA Triplex (31.5 μM) in the presence of different concentrations of each metal complex. The data were presented as $(A - A_0)/(A_f - A_0)$ vs T (T = temperature}, where A_f, A_0, and A, respectively, are the final, the initial, and the observed absorbance at 260 nm. The thermal melting temperature (T_m) was obtained from the first derivative curve ($d\alpha/dT$) ($\alpha = (A - A_0)/(A_f - A_0)$).[19c]

Theoretical Calculations. The structural schematic diagrams of the two metal complexes are given in Figure 1. The general structure of each metal complex contains a Ru(II) ion, two ancillary ligands (bpy or phen), and a intercalative ligand uip. Calculations on the two metal complexes with DFT methods were carried out according to the reported procedures.[38,39]

RESULTS AND DISCUSSION

Electronic Absorption Spectral Studies. Electronic absorption spectroscopy is an effective method to study the interactions of small molecules with RNA triplexes.[40] Aromatic molecules binding with triplexes through intercalation usually result in hypochromism and bathochromism, due to the intercalative mode involving $\pi-\pi$ stacking interactions between an aromatic chromophore and the base pairs of triplexes.[41] The extent of hypochromism commonly parallels the binding strength. Therefore, spectroscopic measurements were first carried out.

Figure 2 shows representative absorption spectra for the two metal complexes in the presence of the triplex poly(U)•poly(A)*poly(U). The quantitative data on the binding are listed in Table 1. The absorption spectra of the triplex are subtracted from those of the mixtures. The two metal complexes exhibit hypochromism throughout the entire absorption region upon binding to the triplex. In the metal to ligand charge transfer region (MLCT band) and the intraligand (IL) uip absorption bands, no obvious red-shifts are observed for the two metal complexes. Compared with Ru**1**, however, more obvious hypochromism in the MLCT and IL bands of Ru**2** at 265 and 455 nm (Figure 2B) indicates stronger interaction between the nucleobases and Ru**2**.[25a,27]

To quantitatively compare the associations of the two complexes with the triplex, the intrinsic binding constants (K_b) and binding site size (s) are determined by monitoring the absorption changes at the MLCT bands. The K_b and s values of Ru**1** are $(6.96 \pm 0.18) \times 10^5$ M^{-1} and 1.41 ± 0.08, respectively, whereas the corresponding values of Ru**2** are $(13.54 \pm 2.23) \times 10^5$ M^{-1} and 1.09 ± 0.03, respectively. A remarkably higher K_b of Ru**2**−triplex suggests a higher binding affinity of Ru**2** with the triplex. A rather modest, smaller binding site size (s) further suggests closer binding site for Ru**2**−triplex interaction, indicating stronger association of Ru**2** to the triplex compared

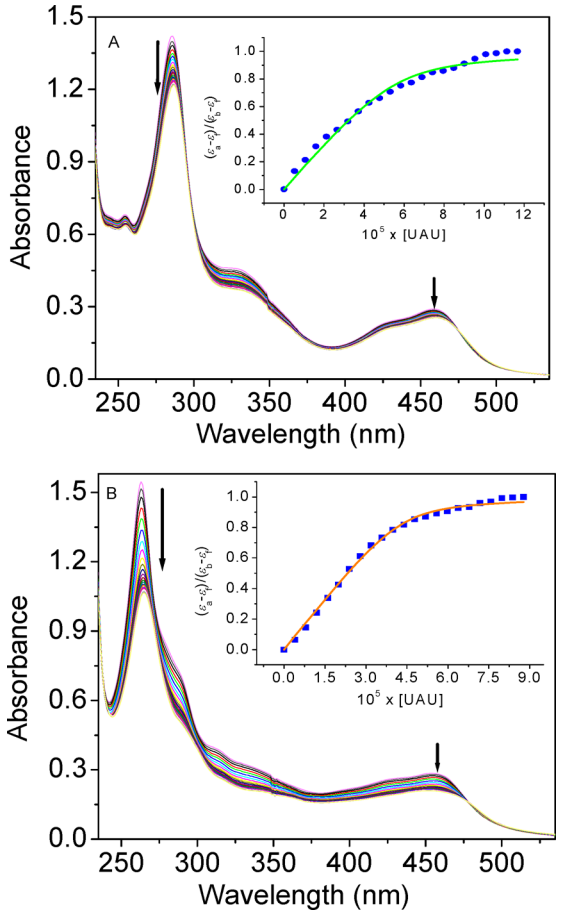

Figure 2. Representative absorption spectral changes of Ru**1** (A) and Ru**2** (B) in the presence of RNA triplex in phosphate buffer (6 mmol/L Na_2HPO_4, 2 mmol/L NaH_2PO_4, 1 mmol/L Na_2EDTA, 19 mmol/L NaC1, pH 7.0) at 20 °C. [Ru**1**] = [Ru**2**] = 20 μM. For Ru1 and Ru2,UAU] = 0−87.7 and 0−116.6 μM, respectively. Where UAU stands for the poly(U)•poly(A)*poly(U). The arrows show the absorbance change upon an increasing poly(U)•poly(A)*poly(U) concentration. Inset: plots of $(\varepsilon_a - \varepsilon_b)/(\varepsilon_f - \varepsilon_b)$ vs [UAU] by nonlinear fit.

with Ru**1**. In addition, the K_b values of the two complexes are rather higher than that of the metal complex PtPR $(1.3 \times 10^4$ $M^{-1})$, which binds to the triplex by a partial intercalation mode.[19b] Interestingly, the K_b value of Ru**1** has the same order of magnitude as those reported for the triplex−alkaloid interactions, such as berberine $((1.6 \pm 0.40) \times 10^5$ $M^{-1})$ and palmatine $((8.0 \pm 0.30) \times 10^5$ $M^{-1})$.[25a] Concerning berberine and palmatine, both bind to the triplex by partial intercalation too. Interestingly, the K_b value of Ru**2** has the same order of magnitude as that of the so-called triplex−intercalator, coralyne $[(4.0 \pm 0.60) \times 10^6$ $M^{-1}]$.[25a] These indicate that the sizes and shapes of small molecules have significant effects on the triplex binding affinities.

Emission Titration. Luminescence measurement was performed to further determine the binding sensitivity of the two metal complexes to the triplex poly(U)•poly(A)*poly(U) in phosphate buffer at 20 °C. The representative spectral profiles of both complexes in the presence of the triplex are shown in Figure 3. Both complexes are strongly fluorescent molecules displaying emission spectra in the 510−790 nm range when excited at 470 nm. Binding to CT-DNA and topoisomerase II is known to remarkably enhance the

dx.doi.org/10.1021/ic5017565 | Inorg. Chem. 2014, 53, 11152−11159

Table 1. Binding Constants (K_b), Average Binding Site Size (s), Hypochromicity (H), and Bathochromic Shifts ($\Delta\lambda$) of Ru1 and Ru2

complex	$\lambda_{max,\ free}$ (nm)	$\lambda_{max,\ bound}$ (nm)	$\Delta\lambda^a$ (nm)	H^b (%)	$K_b{}^c$ ($\times 10^6$ M^{-1})	s^d
Ru**1**	286	287	1	14.1	–	–
	459	460	1	12.4	6.96 ± 0.18	1.41 ± 0.08
Ru**2**	263	265	2	31.0	–	–
	455	457	2	26.4	13.54 ± 2.23	1.09 ± 0.03

[a] $\Delta\lambda$ represents the difference in wavelength of the IL and MLCT band of the metal complex between free and completely bound DNA states. [b] $H = 100 \times (A_{free} - A_{bound})/A_{free}$ (A is the absorbance). [c] K_b was determined by monitoring the changes of absorption at the IL and MLCT bands. [d] s is an average binding size.

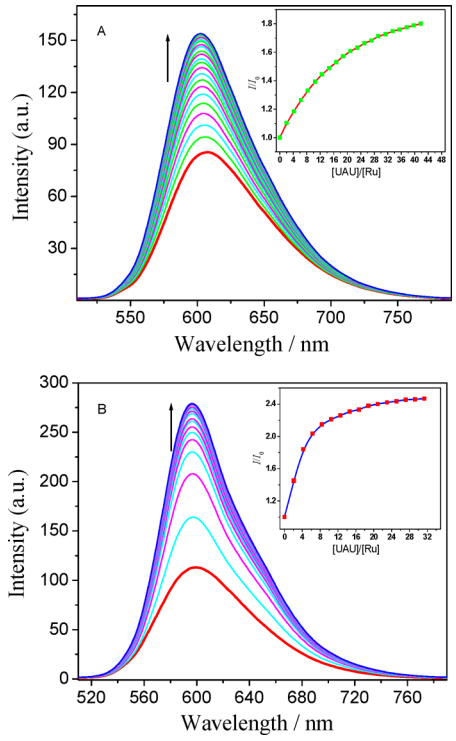

Figure 3. Representative fluorescence emission spectra of Ru**1** (A) and Ru**2** (B) treated with poly(U)•poly(A)*poly(U). [Ru**1**] = [Ru**2**] = 2.0 uM, [UAU] = 0–87.8 μM. The arrows show the intensity increase upon increasing the triplex concentration. Solution conditions are the same as those described in the legend of Figure 2.

fluorescence intensity of Ru**1**.[30] Binding to the triplex also results in an enhancement of the fluorescence of the complexed Ru**1** and Ru**2**, respectively, with 1.8 and 2.5 times that of the triplex-free Ru**1** and Ru**2**. The greater changes of fluorescence intensity suggest a stronger association of Ru**2** with the triplex, resulting from a more effective overlap of the bound molecules with the base triplets.[25a] The result also indicates that the location of the two bound metal complexes is in a hydrophobic environment similar to an intercalated state and Ru**2** is protected more efficiently by the triplex than Ru**2**. Therefore, the accessibility of water molecules to Ru**2** in the presence of the triplex is more difficult in comparison with Ru**1**, leading to Ru**2** displaying a greater emission increase than Ru**1** upon binding to the triplex in saturation state.

Binding Mode by Viscosity Studies. It is well established that the viscometric technique is a reliable hydrodynamic method for investigating the extension of the DNA/RNA helix associated with intercalation.[42] In general, the viscosity of a rodlike nucleic acid increases upon complexation with an intercalator, which is because the axial length of the nucleic acid is enhanced and the helix becomes more rigid.[43] To further study the binding modes of the two metal complexes with the RNA triplex poly(U)•poly(A)*poly(U), the viscosity of the triplex solution has been measured. Figure 4 shows the value of

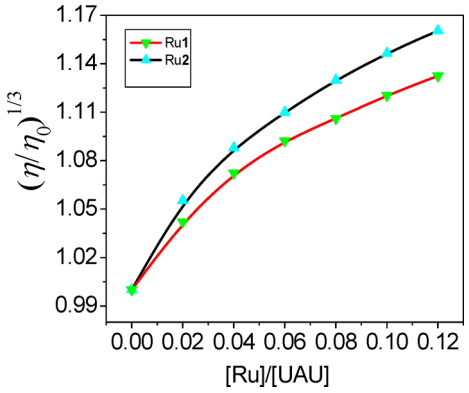

Figure 4. Viscometric Ru**1** and Ru**2** titrations of poly(U)•poly(A)*poly(U) at 20 °C. [UAU] = 107.1 μM. Solution conditions are the same as those described in the legend of Figure 2.

the relative viscosity ratio, η/η_0, as a function of C_{Ru}/C_{UAU} (Ru stands for either Ru**1** or Ru**2**; UAU stands poly(U)•poly(A)*poly(U)). As can be seen from Figure 4, the viscosity of both poly(U)•poly(A)*poly(U)–Ru**1** and –Ru**2** systems increases with C_{Ru}/C_{UAU}, tending to level off at the highest values of this ratio. The observed trend suggests that the two metal complexes bind to the triplex by intercalation. However, the overall viscosity variation of the poly(U)•poly(A)*poly(U)–Ru**1** system is somewhat more modest than that of poly(U)•poly(A)*poly(U)–Ru**2**. The reason for this may be that the enhanced rigidity of the triple strand by Ru**1** is relatively smaller than that by Ru**2**, which results in the triplex being less sensitive to the structural modifications that arise from Ru**1** binding. Notably, in the binding mode besides intercalation, another complex is likely formed in the course of each metal complex binding to the triplex, where the metal complex assembles on the polymer surface in such a way that the chain length displays no appreciable changes.

Fluorescence Quenching Experiments. Steady-state emission quenching experiments may provide more information about small molecules binding to the RNA triplex. Concerning the complex of the triplex–small molecules, small molecules that are free or bound on the surface of the triple helix are readily available to the quencher, whereas those that are intercalated into base triplets are not. In addition, the electrostatic barrier resulting from the negative charges on the phosphate groups at the helix surface may prevent the anionic quencher from further penetration into the interior of the helix.

dx.doi.org/10.1021/ic5017565 | Inorg. Chem. 2014, 53, 11152–11159

Therefore, if the binding involves intercalation, the emission of the triplex–small molecule system will display little or no quenching upon the addition of anionic quencher. Consequently, the quenching constants (K_{sv}) of small molecules bound to the triplex by intercalation are smaller than those of small molecules alone. Figure 5 presents the effects of anionic

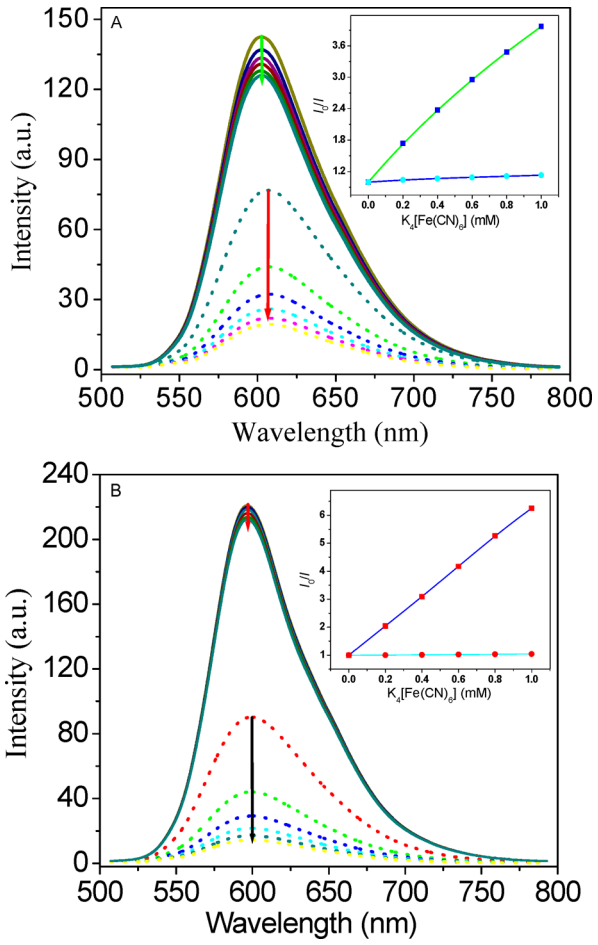

Figure 5. Fluorescence quenching of Ru**1** (A) and Ru**2** (B) in the absence (dotted lines) and in the presence (solid lines) of the triplex by $[Fe(CN)_6]^{4-}$. [Ru**1**] = [Ru**2**] = 20 μM, [UAU]/[Ru] = 314, $[Fe(CN)_6]^{4-}$ = 0–1.0 mM. The arrows show the intensity decrease upon an increasing the triplex concentration. Inset: plots of I_0/I vs $[Fe(CN)_6]^{4-}$, where I_0 and I are the fluorescence intensities in the absence and presence of the quencher, respectively. K^+ concentration of each system is kept a constant using KCl. Solution conditions are the same as those described in the legend of Figure 2.

quencher $[Fe(CN)_6]^{4-}$ on the fluorescence intensity of each metal complex in the absence and presence of the triplex poly(U)•poly(A)*poly(U). As shown in Figure 5, the emissions of Ru**1** and Ru**2** in the absence of the triplex were almost completely quenched by $[Fe(CN)_6]^{4-}$ with K_{sv} values of 2950 and 5290 L mol^{-1}, respectively. However, the emissions of Ru**1** and Ru**2** in the presence of the triplex display no obvious quenching, respectively, with K_{sv} values of 130 and 43 L mol^{-1}. The result indicates that binding of the two metal complexes with the triplex may decrease to some extent the accessibility of the anionic quencher $[Fe(CN)_6]^{4-}$ to each bound metal complex, suggesting that the binding mode of each metal complex with the triplex is intercalation. In comparison with Ru**1**, a smaller K_{sv} for Ru**2** in the presence of the triplex is indicative of a stronger association of Ru**2** with the triplex, resulting presumably from a more effective overlap of the bound Ru**2** with the base triplets.

Thermal Denaturation Studies. Dissociation (denaturation) of a triplex nucleic acid into a duplex plus a single strand results in significant hyperchromism around 260 nm.[29a] Binding of a small molecule to a triplex nucleic acid alters the denaturation temperatures (T_m) depending on the strength of its interactions with the different triplex nucleic acid conformations. Small molecules as intercalators as well as the neutralization of the negative charges on the phosphate groups may enhance the denaturation temperature of a triplex nucleic acid. Furthermore, the binding specificity of small molecules to the Hoogsteen base-paired third strand or to the Watson–Crick base-paired duplex can be readily discriminated.[29a] Hence, thermal denaturation profiles provide a convenient means for detecting binding and also assessing relative binding strengths.

Under the conditions used in this study, the melting profile of free triple-helical poly(U)•poly(A)*poly(U) is biphasic (Figure 6A and B, red curve). The first T_m (T_{m1}) occurring at about 37.6 °C is assigned to the transition of poly(U)•poly(A)*poly(U) triplex to poly(U)•poly(A) duplex and single-stranded poly(U) via dissociation of the Hoogsteen base-paired poly(U) strand from the major groove of the template duplex.[22,27] The higher T_m (T_{m2}) occurring at about 45.5 °C

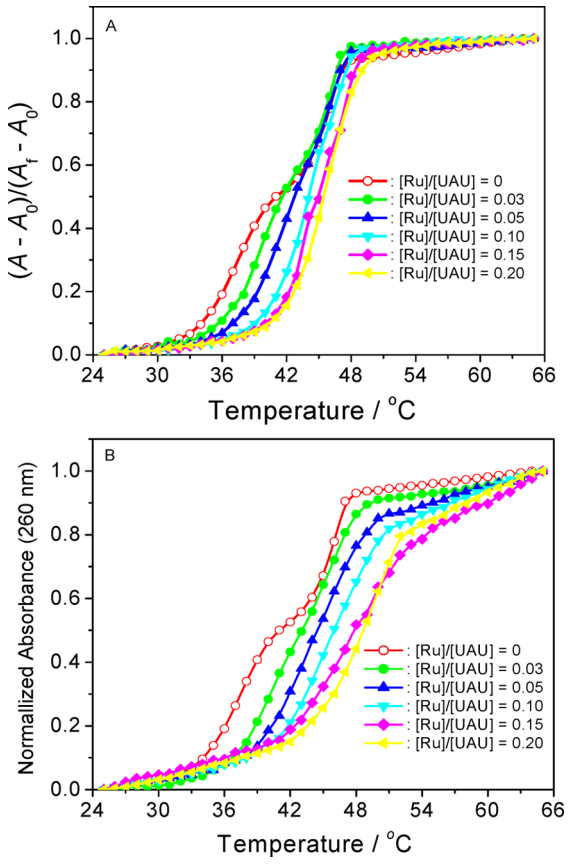

Figure 6. Melting curves at 260 nm of poly(U)•poly(A)*poly(U) (31.5 μM) and its complexation with Ru**1** (A) and Ru**2** (B) at different [Ru]/[UAU] ratios, where A_f, A_0, and A are the final, the initial, and the observed absorbance at 260 nm, respectively. Solution conditions are the same as those described in the legend of Figure 2, and $[Na^+]$ = 35 mM.

dx.doi.org/10.1021/ic5017565 | Inorg. Chem. 2014, 53, 11152–11159

corresponds to the dissociation of the Watson–Crick base-paired duplex poly(U)•poly(A). Binding of each metal complex results in both melting temperatures being raised to varying extents (Figure 6 and Table 2), whereas the effect of

Table 2. Melting Temperature (°C) of the Triplex Poly(U)•Poly(A)*Poly(U) in the Absence and Presence of Ru1 and Ru2, Respectively[a]

triplex/complex	[Ru]/[UAU]	T_{m1} (°C)	T_{m2} (°C)	ΔT_{m1} (°C)	ΔT_{m2} (°C)
RNA triplex	0	37.6	45.5	–	–
RNA triplex + Ru**1**	0.03	40.0	45.5	2.4	0.0
	0.05	41.7	45.7	4.1	0.2
	0.10	44.0	47.0	6.4	1.5
	0.15	43.6	47.5	7.0	2.0
	0.20	46.1	–	8.5	–
RNA triplex + Ru**2**	0.03	40.5	45.7	2.9	0.2
	0.05	43.1	45.9	5.5	0.4
	0.10	45.0	47.9	7.4	2.4
	0.15	47.0	49.9	9.4	4.4
	0.20	50.0	–	12.4	–

[a] $[Na^+]$ = 35 mM.

Ru**1** on the stabilization of the third strand is somewhat less than with Ru**2** but is still strong enough to raise the first T_m to 46.1 °C. In the presence of Ru**2**, however, the effect is so strong that dissociation of the third strand does not occur before duplex dissociation, so that only a single broad transition is observed at 50.0 °C. The results indicate that the two metal complexes bind to the triplex structure more strongly than to the duplex structure under the same condition, resulting in a specific stabilization of the triplex structure. Therefore, we propose that the ligand uip in each metal complex is intercalated with the two ancillary ligands (bpy or phen) located in the minor groove of the polynucleotide, thereby stabilizing the third strand by expansion of the stacking interaction.[29a] Interestingly, the effects of the two metal complexes on the stabilization of the triplex poly(U)•poly(A)*poly(U) are different from what has been reported in the presence of some triplex binders, such as ethidium (EB),[19a] proflavine (PR), and its metal complex Pt-proflavine (PtPR),[19c] where EB, PR, and PtPR exert a stabilization effect on the duplex structure and definitely destabilize the triplex structure. Furthermore, the effects of the two metal complexes on the triplex stabilization are different from what has been observed in the presence of alkaloids berberine, palmatine, and coralyne.[25a] With regard to berberine, palmatine, and coralyne, these alkaloids stabilize the third strand without affecting the stabilization of the duplex. Recent studies of the interaction mechanisms of coralyne with poly(U)•poly(A)*poly(U) reflect that coralyne tends to stabilize the triplex structure because of this small molecule being able to induce the triplex-to-duplex conversion and also the duplex-to-triplex conversion.[23] These further reveal that the effects of small molecules on the stabilization of RNA triplexes are complicated and sensitive to their structural features and interaction processes.

Conformational Aspects of the Binding. Conformational changes of the RNA triplex poly(U)•poly(A)*poly(U) reduced by the two metal complexes were investigated by intrinsic circular dichroic studies (Figure 7). The circular dichroic spectrum of the free RNA triplex (Figure 7A) is characterized by a large positive band at about 260 nm and an

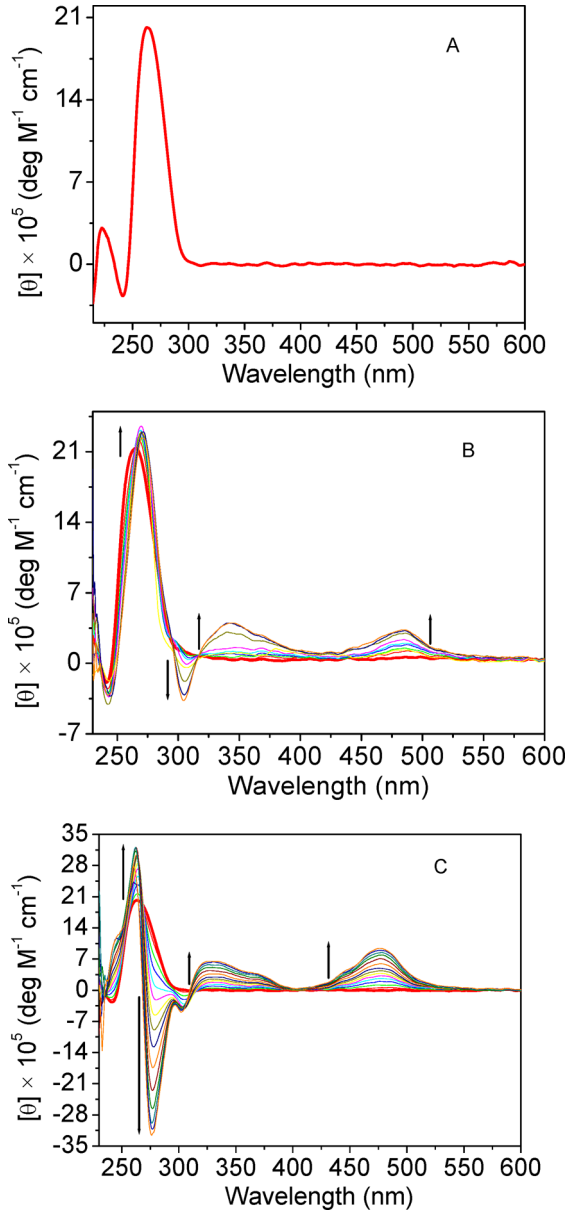

Figure 7. CD spectra of poly(U)•poly(A)*poly(U) (A, 100 μM) treated with either Ru**1** (B) or Ru**2** (C) at different [Ru]/[UAU] ratios from 0 to 0.09 or 0 to 0.28, respectively. Solution conditions are the same as those described in the legend of Figure 2.

adjacent weak negative band at about 240 nm followed by a small positive band at about 220 nm.[13] In addition, the two metal complexes display no intrinsic CD signals because both are racemic compounds. Concerning the triplex–Ru**1** (Figure 7B) and triplex–Ru**2** (Figure 7C) systems; therefore, any CD signals occurring above 300 nm are attributed to the metal complex induced by the triplex, and the changes below 300 nm result from either the triplex perturbation induced by the metal complex or the metal complex induced by the triplex.[44] As can be seen from Figure 7, binding of each metal complex with the triplex results in hyperchromic effects on the most energetic band at 260 nm and formations of three new bands above 275 nm. These suggest that both metal complexes could bind to the chiral environment of the RNA triplex via interaction. In the presence of Ru**2**, however, the hyperchromic effect at 260 nm is more remarkable. With Ru**1**, two new positive bands occur,

dx.doi.org/10.1021/ic5017565 | Inorg. Chem. 2014, 53, 11152–11159

respectively, at about 340 and 484 nm, and a new negative band occurs at about 304 nm. In the presence of Ru**2**, the new positive g bands occur, respectively, at aroundt 326 and 476 nm, and the new negative band is observed at about 276 nm. Furthermore, the intensities of the new bands of the triplex−Ru**2** system are rather higher than that of the triplex−Ru**1** system, suggesting stronger association of Ru**2** with the triplex.

Explanations for the Interaction Differences of the Two Metal Complexes with Triplex. The above analyses indicate that the association of Ru**2** with the triplex is stronger than that of Ru**2**. Consequently, Ru**2** stabilizing the third strand is more effective than Ru**1**. Although the mechanism of the triplex poly(U)•poly(A)*poly(U) stabilization by the two metal complexes is not clear, we try add an analysis from the following respects.

(i). Effect of the Aromatic Planarity of Intercalative Ligand. Previous studies suggest that the aromatic planarity of intercalative ligand play key roles in governing the binding behaviors of small molecules with triplexes.[25a,29a] In general, good stacking interactions between the base triplets and the intercalator obviously enhance the triplex stabilization.[29a] Apparently, the uip moiety is an important feature for introducing intercalation properties to the two metal complexes. Although the crystal structures of the two metal complexes have not been obtained here, the DFT-optimized structures show that the planarities of the intercalative ligands uip in the two metal complexes are almost the same: for uip in Ru**1** and Ru**2**, the dihedral angles of N(7)−C(8)−C(9)−C(10) are 0.0139° and 0.3122°, respectively; no obvious differences exist in the planarities of intercalative ligands uip, reflecting that the planarities of the intercalative ligands uip in the two metal complexes are almost the same. Thus, we presume that the planarities of intercalative ligands may not be the main factor resulting in the interaction differences of the two metal complexes with the triplex.

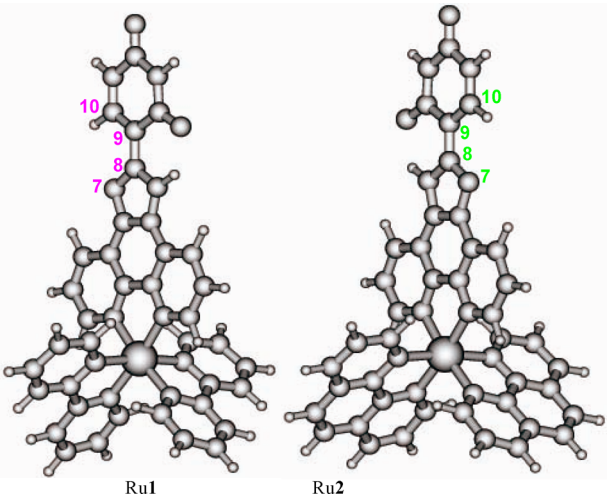

Figure 8. DFT-optimized structures and visualization of the orbitals of complexes Ru**1** (left) and Ru**2** (right).

(ii). Effect of Intermolecular Hydrogen Bond. The intercalative ligand uip in the two complexes contains imino functional groups, which could possibly form intermolecular hydrogen bonds with the base pairs of the triplex poly(U)•poly(A)*poly(U). However, previous studies on the acridine derivatives−triplex DNA interactions confirmed that intermolecular hydrogen bonds did not significantly affect the stabilization of triplexes,[45] and similar behaviors were further observed for $[Ru(II)(1,10\text{-phenanthroline})_2L]^{2+}$ complexes.[29a] Therefore, we presume that the role of hydrogen bond formation between the intercalator (Ru**1** or Ru**2**) and the third strand is likely to be a minor factor effect on the triplex stabilization.

(iii). Polarity Effect. The separation of negative backbone charges inherent to intercalation may help to overcome unfavorable electrostatics for third-strand association.[25a,29a] However, the cationic natures of two metal complexes are the same. Thus, both polarity effects of the triplex and electron transfer from the base triplets to the metal complex may not be the main factor contributing to the differences of the third-strand stabilization.

(iv). Effect of the Hydrophobicity of the Ancillary Ruthenium Ligand. The binding reaction of small molecule with nucleic acids is driven primarily by hydrophobic interactions.[46] As the ancillary ligand progresses from bpy to phen studied, the bulkiness and hydrophobic character of this ligand is increased. Consequently, the hydrophobic transfer of the large aromatic complex Ru**2** from solution into the triplex binding site caused by the ancillary ligand phen is easier to achieve, resulting in the binding sites effectively overlapping with each other. This can also be confirmed by a smaller binding site size (1.09 ± 0.03) of Ru**2** from UV−visible titration data, and emphasizes that small differences in ancillary ligand structure have significant effect on the triplex interaction. Therefore, the effects of ancillary ligands (bpy and phen) on the binding characteristics of the two metal complexes with the triplex should not be ignored, which is likely the main factor affecting the interactions of the two metal complexes with the triplex.

■ CONCLUSIONS

This work presents the comparative binding of the RNA triplex poly(U)•poly(A)*poly(U) with Ru**1** and Ru**2** using various biophysical techniques. The studies reveal that the two metal complexes bind to the RNA triplex by intercalation and stabilize the Hoogsteen base-paired third strand. However, the binding affinity of the RNA triplex with Ru**2** is greater than that with Ru**1**, which results in Ru**2** exerting a rather remarkable stabilization effect on the triplex structure. The extra hydrophobic area represented by the fused benzene ring of phenanthroline does seem to not only influence the intrinsic binding constants, but also influence the third-strand stabilization. Considering the structural characteristics of the two metal complexes, we presume that the hydrophobicity effects of ancillary ligands may likely contribute to the binding differences of Ru**1** and Ru**2** with the RNA triplex. This study further advances our knowledge on the binding of the RNA triplex with metal complexes, particularly octahedral ruthenium(II) polypyridyl complexes.

■ ASSOCIATED CONTENT

Ⓢ Supporting Information

NMR spectra and Maldi-Tof-MS of Ru2. This material is available free of charge via the Internet at http://pubs.acs.org.

■ AUTHOR INFORMATION

Corresponding Author

*E-mail: lfwyxh@yeah.net, lfwyxh@yahoo.com.cn. Fax: +86 731 58293997.

Notes

The authors declare no competing financial interest.

■ ACKNOWLEDGMENTS

This work was supported by the National Natural Science Foundation of China (21071120 and 21371146), Hunan Provincial Natural Science Foundation of China (12JJ2011) and the Key Project of Chinese Ministry of Education (212127).

■ REFERENCES

(1) Felsenfeld, G.; Davies, D. R.; Rich, A. *J. Am. Chem. Soc.* **1957**, *79*, 2023−2024.
(2) (a) Stevens, C. L.; Felsenfeld, G. *Biopolymers* **1964**, *2*, 293−314. (b) MMichelson, A. M.; Monny, C. *Biochim. Biophys. Acta* **1967**, *149*, 107−126. (c) Mills, M.; Arimondo, P. B.; Lacroix, L.; Garestier, T.; Helene, C.; Klump, H.; Mergny, J. L. *J. Mol. Biol.* **1999**, *291*, 1035−54. (d) Mills, M.; Arimondo, P. B.; Lacroix, L.; Garestier, T. S.; Klump, H.; Mergny, J. L. *Biochemistry* **2002**, *41*, 357−366.
(3) (a) Mirkin, S. M.; Lyamichev, V. I.; Drushlak, K. N.; Dobrynin, V. N.; Filippov, S. A.; Frank−Kamenetskii, M. D. *Nature* **1987**, *330*, 495−497. (b) Hanvey, J. C.; Shimizu; Wells, R. D. *Proc. Natl. Acad. Sci. U.S.A.* **1988**, *85*, 6292−6296. (c) Wells, R. D.; Collier, D. A.; Shimizu; Wohlrab, F. *FASEB J.* **1988**, *2*, 2939−2949.
(4) Cooney, M.; Czernuszewicz, G.; Postel, E. H.; Flint, S. J.; Hogan, M. E. *Science* **1988**, *241*, 456−459.
(5) Thuong, N. T.; Helene, C. *Angew. Chem., Int. Ed.* **1993**, *32*, 666−690.
(6) Sun, J. S.; Helene, C. *Curr. Opin. Struct. Biol.* **1993**, *3*, 345−356.
(7) Kinniburgh, A. J.; Firulli, A. B.; Kolluri, R. *Gene* **1994**, *149*, 93−100.
(8) Buckin, V.; Tran, H.; Morozov, V.; Marky, L. A. *J. Am. Chem. Soc.* **1996**, *118*, 7033−7039.
(9) Aboulela, F.; Karn, J.; Varani, G. *J. Mol. Biol.* **1995**, *253*, 313−332.
(10) Dinman, J. D.; Richter, S.; Plant, E. P.; Taylor, R. C.; Hammell, A. B.; Rana, T. M. *Proc. Natl. Acad. Sci. U.S.A.* **2002**, *99*, 5331−5336.
(11) Jain, A.; Bacolla, A.; Chakraborty, P.; Grosse, F.; Vasquez, K. M. *Biochemistry* **2010**, *49*, 6992−6999.
(12) Buske, F. A.; Mattick, J. S.; Bailey, T. L. *RNA Biol.* **2011**, *8*, 427−439.
(13) Das, S.; Kumar, G. S.; Ray, A.; Maiti, M. *J. Biomol. Struct. Dyn.* **2003**, *20*, 703−714.
(14) Christensen, L. A.; Finch, R. A.; Booker, A. J.; Vasquez, K. M. *Cancer Res.* **2006**, *66*, 4089−4094.
(15) (a) Li, M.; Zengeya, T.; Rozners, E. *J. Am. Chem. Soc.* **2010**, *132*, 8676−8681. (b) Gupta, P.; Muse, O.; Rozners, E. *Biochemistry* **2012**, *51*, 63−73.
(16) (a) Lehrman, E. A.; Crothers, D. M. *Nucleic Acids Res.* **1977**, *4*, 1381−1392. (b) Arya, D. P.; Coffee, R. L., Jr.; Charles, I. *J. Am. Chem. Soc.* **2001**, *123*, 11093−11094.
(17) Polak, M.; Hud, N. V. *Nucleic Acids Res.* **2002**, *30*, 983−992.
(18) (a) Arya, D. P.; Micovic, L.; Charles, I.; Coffee, R. L., Jr.; Willis, B.; Xue, L. *J. Am. Chem. Soc.* **2003**, *125*, 3733−3744. (b) Arya, D. P. *Acc. Chem. Res.* **2011**, *44*, 134−146.
(19) (a) Garcia, B.; Leal, J. M.; Paiotta, V.; Ibeas, S.; Ruiz, R.; Secco, F.; Venturini, M. *J. Phys. Chem. B* **2006**, *110*, 16131−16138. (b) García, B.; Leal, J. M.; Paiotta, V.; Ruiz, R.; Secco, F.; Venturini, M. *J. Phys. Chem. B* **2008**, *112*, 7132−7139. (c) Hoyuelos, F. J.; García, B.; Leal, J. M.; Busto, N.; Biver, T.; Secco, F.; Venturinib, M. *Phys. Chem. Chem. Phys.* **2014**, *16*, 6012−6018.
(20) (a) Bhowmik, D.; Kumar, G. S. *Mol. Biol. Rep.* **2013**, *40*, 5439−5450. (b) Bhowmik, D.; Das, S.; Hossain, M.; Haq, L.; Kumar, G. S. *PLoS One* **2012**, *7*, e37939−e37939.
(21) Ben, G. N.; Chao, Z.; Gerrard, S. R.; Fox, K. R.; Brown, T. *ChemBioChem* **2009**, *10*, 1839−1851.
(22) Doluca, O.; Boutorine, A. S.; Filichev, V. V. *ChemBioChem* **2011**, *12*, 2365−2374.
(23) Lozano, H. J.; García, B.; Busto, N.; Leal, J. M. *J. Phys. Chem. B* **2013**, *117*, 38−48.
(24) Tan, L. F.; Xie, L. J.; Sun, X. N. *J. Biol. Inorg. Chem.* **2013**, *18*, 71−80.
(25) (a) Sinha, R.; Kumar, G. S. *J. Phys. Chem. B* **2009**, *113*, 13410−13420. (b) Xi, H. J.; Davis, E.; Ranjan, N.; Xue, L.; Hyde-Volpe, D.; Arya, D. P. *Biochemistry* **2011**, *50*, 9088−91113.
(26) Shchyolkina, A. K.; Timofeev, E. N.; Lysov, Y. P.; Florentiev, V. L.; Jovin, T. M.; Arndt-Jovin, D. J. *Nucleic Acids Res.* **2001**, *29*, 986−995.
(27) Tan, L. F.; Liu, J.; Shen, J. L.; Liu, X. H.; Zeng, L. L.; Jin, L. H. *Inorg. Chem.* **2012**, *51*, 4417−4419.
(28) (a) Erkkila, K. E.; Odom, D. T.; Barton, J. K. *Chem. Rev.* **1999**, *99*, 2777−2795. (b) Ji, L. N.; Zou, X. H.; Liu, J. G. *Coord. Chem. Rev.* **2001**, *216*−*217*, 513−536. (c) Genereux, J. C.; Barton, J. K. *Chem. Rev.* **2010**, *110*, 1642−1662.
(29) (a) Choi, S. D.; Kim, M. S.; Kim, S. K.; Lincoln, P.; Tuite, E.; Nordén, B. *Biochemistry* **1997**, *36*, 214−223. (b) Lim, A. C.; Barton, J. K. *Biochemistry* **1998**, *37*, 9138−9146.
(30) Gao, F.; Chao, H.; Wang, J. Q.; Yuan, Y. X.; Sun, B.; Wei, Y. F.; Peng, B.; Ji, L. N. *J. Biol. Inorg. Chem.* **2007**, *12*, 1015−1027.
(31) Yamada, M.; Tanaka, Y.; Yoshimato, Y.; Kuroda, S.; Shimao, I. *Bull. Chem. Soc. Jpn.* **1992**, *65*, 1006−1011.
(32) Sullivan, B. P.; Sullivan, D. J.; Meyer, T. J. *Inorg. Chem.* **1978**, *17*, 3334−3341.
(33) Tan, L. F.; Xie, L. J.; Sun, X. N.; Zen, L. L.; Yang, G. *J. Inorg. Biochem.* **2013**, *120*, 32−38.
(34) Buckin, V.; Tran, H.; Morozov, V.; Marky, L. A. *J. Am. Chem. Soc.* **1996**, *118*, 7033−7039.
(35) Sinha, R.; Kumar, G. S. *J. Phys. Chem. B* **2009**, *113*, 13410−13420.
(36) Carter, M. T.; Rodriguez, M.; Bard, A. J. *J. Am. Chem. Soc.* **1989**, *111*, 8901−8911.
(37) Lakowicz, J. R.; Webber, G. *Biochemistry* **1973**, *12*, 4161−4170.
(38) Cohen, G.; Eisenberg, H. *Biopolymers* **1969**, *8*, 4549−4560.
(39) Tan, L. F.; Shen, J. L.; Liu, J.; Zeng, L.L; Jin, L. H.; Weng, C. *Dalton Trans.* **2012**, *41*, 4575−4587.
(40) (a) Faria, M.; Wood, C. D.; Perrouault, L.; Nelson, J. S.; Winter, A.; White, M. R. H.; Hélène, C.; Giovannangeli, C. *Proc. Natl. Acad. Sci. U.S.A.* **2000**, *97*, 3862−3867. (b) Vuyisich, M.; Beal, P. A. *Nucleic Acids Res.* **2000**, *28*, 2369−2374.
(41) Kabir, A.; Kumar, G. S. *Mol. BioSyst.* **2014**, *10*, 1172−1183.
(42) Satyanarayana, S.; Dabrowiak, J. C.; Chaires, J. B. *Biochemistry.* **1993**, *32*, 2573−2584.
(43) Lerman, L. S. *J. Mol. Biol.* **1961**, *3*, 18.
(44) Tijana, B.; Olga, N.; Anna, H.; Lenka, Z.; Oldrich, V.; Jana, K.; Abraha, H.; Simon, P.; Peter, J. S.; Viktor, B. *J. Med. Chem.* **2008**, *51*, 5310−5319.
(45) Kim, H. K.; Kim, J. M.; Kim, S. K.; Rodger, A.; Nordén, B. *Biochemistry* **1996**, *35*, 1187−1194.
(46) (a) Haq, I.; Lincoln, P.; Suh, D.; Norden, B.; Chowdhry, B. Z.; Chaires, J. B. *J. Am. Chem. Soc.* **1995**, *117*, 4788−4796. (b) Vandiver, M. S.; Bridges, E. P.; Koon, R. L.; Kinnaird, A. N.; Glaeser, J. W.; Campbell, J. F.; Priedemann, C. J.; Rosenblatt, W. T.; Herbert, B. J.; Wheeler, S. K.; Wheeler, J. F.; Kane-Maguire, N. A. P. *Inorg. Chem.* **2010**, *49*, 839−848.